Recombinant Viral-Vectored Vaccines Expressing *Plasmodium chabaudi* AS Apical Membrane Antigen 1: Mechanisms of Vaccine-Induced Blood-Stage Protection

Sumi Biswas,* Alexandra J. Spencer,* Emily K. Forbes,* Sarah C. Gilbert,*
Anthony A. Holder,[†] Adrian V. S. Hill,* and Simon J. Draper*

Apical membrane Ag 1 (AMA1) is one of the leading candidate Ags for inclusion in a subunit vaccine against blood-stage malaria. However, the efficacy of Ab-inducing recombinant AMA1 protein vaccines in phase IIa/b clinical trials remains disappointing. In this article, we describe the development of recombinant human adenovirus serotype 5 and modified vaccinia virus Ankara vectors encoding AMA1 from the *Plasmodium chabaudi chabaudi* strain AS. These vectors, when used in a heterologous prime-boost regimen in BALB/c mice, are capable of inducing strong transgene-specific humoral and cellular immune responses. We show that this vaccination regimen is protective against a nonlethal *P. chabaudi chabaudi* strain AS blood-stage challenge, resulting in reduced peak parasitemias. The role of vaccine-induced, AMA1-specific Abs and T cells in mediating the antiparasite effect was investigated by in vivo depletion of CD4+ T cells and adoptive-transfer studies into naive and immunodeficient mice. Depletion of CD4+ T cells led to a loss of vaccine-induced protection. Adoptive-transfer studies confirmed that efficacy is mediated by both CD4+ T cells and Abs functioning in the context of an intact immune system. Unlike previous studies, these results confirm that Ag-specific CD4+ T cells, induced by a clinically relevant vaccine-delivery platform, can make a significant contribution to vaccine blood-stage efficacy in the *P. chabaudi* model. Given that cell-mediated immunity may also contribute to parasite control in human malaria, these data support the clinical development of viral-vectored vaccines that induce both T cell and Abs against *Plasmodium falciparum* blood-stage malaria Ags like AMA1.   *The Journal of Immunology*, 2012, 188: 5041–5053.

M alaria remains a significant burden on global public health, despite some recent and encouraging successes with regard to malaria control in certain parts of Africa. Thus, the development of a highly effective vaccine, which could help in the control and eventual elimination of this disease, remains an important goal (1). Vaccines against the asexual blood-stage of malaria infection have often aimed to reproduce natural immunity and have generally targeted Ags associated with the merozoite surface or located in the apical organelles (2). Apical membrane Ag 1 (AMA1) appears on the surface of merozoites after its release from the micronemes, where it is a target of growth-inhibitory Abs in in vitro assays and in vivo malaria models. It is also frequently associated with naturally acquired immunity and, thus, has classically been one of the leading candidate Ags for inclusion in a subunit vaccine against the asexual blood-stage of the parasite (3). In an attempt to induce such protective Abs, malaria vaccine developers have classically focused on recombinant protein-in-adjuvant vaccines. Typically, these require multiple immunizations in animal models to induce Ab responses of a protective magnitude (4), and clinical trials of the efficacy of such candidate vaccines remain disappointing (2).

An increasingly recognized alternative to protein-in-adjuvant formulations is the use of viral-vectored vaccines (5, 6) and, in particular, replication-defective adenoviruses of both human and simian serotype, as well as poxviruses, such as modified vaccinia virus Ankara (MVA). These vectors can express relatively large Ag constructs and, when deployed in an adenovirus-MVA heterologous prime-boost regimen, were shown in mice and nonhuman primates to induce high levels of Ag-specific CD8+ and CD4+ T cell responses, as well as high titers of Ab (7–12). The chimpanzee adenovirus ChAd63 and MVA have both displayed an excellent safety profile for use in humans as prophylactic vaccines (13, 14), and the recombinant adenovirus-MVA vaccine-delivery platform has shown high-level efficacy against all three malaria life-cycle stages in preclinical models (9, 15–17).

There have been numerous studies suggesting that the induction of cellular immunity in conjunction with Ab responses may increase the efficacy of vaccines targeting classical blood-stage Ags, leading to recent calls for such an approach to be tested clinically (18). Studies using both sporozoite and infected RBC inoculation to immunize human volunteers have associated cellular immune responses against blood-stage parasites with protective outcome (19, 20). Similarly, three studies in the *Plasmodium yoelii* mouse

Address correspondence and reprint requests to Dr. Sumi Biswas, Jenner Institute, University of Oxford, Old Road Campus Research Building, Roosevelt Drive, Oxford OX3 7DQ, U.K. E-mail address: sumi.biswas@ndm.ox.ac.uk

model have associated CD8$^+$ T cell responses against blood-stage parasites or the merozoite surface protein 1 (MSP1) Ag with protective immunity against pre-erythrocytic liver-stage infection (7, 21, 22), and a more recent study even associated such CD8$^+$ T cells with protective blood-stage immunity (23). Other studies with *Plasmodium yoelii* have shown that the adoptive transfer of CD4$^+$ T cell lines against Ags, such as MSP1$_{33}$, into naive mice can lead to the control of blood-stage parasitemia (24), although not all vaccinated or T cell-transfused recipients survive, despite a significant reduction in parasite densities. We also reported previously that a human adenovirus serotype 5 (AdHu5)-MVA vaccination regimen against the *P. yoelii* MSP1$_{42}$ Ag can induce strong Ag-specific cellular and humoral immune responses. In this case, the CD8$^+$ T cells against MSP1$_{33}$ provided partial efficacy against developing liver-stage parasites; however, depletion of either the CD8$^+$ or CD4$^+$ T cell subsets prior to blood-stage challenge of immunized mice had no effect on protective outcome (7, 9).

The *Plasmodium chabaudi chabaudi* strain AS parasite has provided an alternative and highly informative model for the study of blood-stage malaria immunity, in which both Abs and CD4$^+$ T cells (acting as helper cells for B cells, as well as through Ab-independent mechanisms) are reported to be important (25). In the case of infection with this parasite, immunologically competent mice generate a protective immune response that involves both Th1 and Th2-type CD4$^+$ T cells (26), with the importance of such cells demonstrated in numerous depletion and adoptive-transfer studies in immunodeficient mice (27). During the acute stage of infection, a Th1-type Ab-independent response has been shown to control initial peak parasitemia, with this effect mediated by the production of proinflammatory cytokines and effector molecules, such as IFN-γ and TNF-α (27). Once parasitemia is brought under control, a Th2-type CD4$^+$ T cell response appears to predominate. These cells were shown to produce IL-4, IL-5, IL-6, and IL-10, as well as to provide essential help for Ab production by B cells (28, 29). B cell-depletion studies showed that these cells per se are not required for early control of parasitemia but are important for the resolution of the chronic phase of infection and the clearance of the parasite (30).

In agreement with these data, immunization studies with recombinant AMA1 in the *P. chabaudi adami* model also showed an important contribution of CD4$^+$ T cells acting independently of Abs in vaccine-induced protection (31). In this study, a significant decrease in acute antiparasite immunity was seen if CD4$^+$ T cells were depleted from immunized normal or B cell knockout mice prior to blood-stage challenge. Similarly, athymic (*nu/nu*) mice transfused with a CD4$^+$ T cell line raised against a conserved cryptic epitope in AMA1 showed 50% survival following *P. chabaudi adami* challenge, and accelerated rates of de novo Ab production against AMA1 in some mice (32). Comparable observations were made in a similar study following adoptive transfer of transgenic CD4$^+$ T cells that recognized a H-2 I-E^d epitope within *P. chabaudi* MSP1$_{33}$ (33). A more recent study showed that low doses of killed blood-stage *P. chabaudi chabaudi* strain AS parasites, administered in aluminum hydroxide adjuvant plus the TLR9 agonist CpG oligodeoxynucleotide, can induce high-level cross-strain, and even some cross-species, immunity that is dependent on CD4$^+$ T cells, IFN-γ, and NO (34). However, none of these studies using recombinant AMA1 protein formulated in Montanide ISA720 adjuvant, transferred CD4$^+$ T cell lines, or transgenic T cells, or a whole-parasite blood product administered with CpG, represent vaccine formulations that are easily translatable with demonstrated adequate safety profiles for human use (35, 36).

In this study, we characterize the immunogenicity and protective efficacy of a prime-boost vaccination regimen with viral-vectored vaccines targeting *P. chabaudi chabaudi* strain AS AMA1 and in-

vestigate the mechanisms of vaccine-induced protection following challenge with *P. chabaudi* blood-stage parasites. These vectors induce AMA1-specific T cell and Ab responses and provide a system in which to dissect the protective contribution of both the cellular and humoral arms of the immune system. Depletion and adoptive-transfer studies demonstrate an important contribution of both vaccine-induced CD4$^+$ T cells and Abs to protective immunity. These data, generated with a vaccine platform that is highly suited for human use (13, 14), support the further clinical translation of this approach. Given the evidence that cell-mediated immunity may also contribute to parasite control in human malaria, the development of viral-vectored vaccines targeting Ags, such as *Plasmodium falciparum* AMA1, which induce strong cellular immune responses in conjunction with Abs, may stand a greater chance of success in protecting humans against blood-stage parasites in comparison with vaccination strategies aiming to induce Abs alone.

Materials and Methods

Generation of viral vectors expressing AMA1

The forward primer (5′-ATG AAA GAA ATA TAT TAT ATT GTA ATT TTG TGC-3′) and reverse primer (5′-TTA ATA GTA TGG TTT TTC CAT CAA AAC TG-3′) were used to amplify the Ag from genomic *P. chabaudi chabaudi* strain AS DNA by PCR, prior to ligation into a plasmid and sequencing. The genomic DNA was obtained from Dr. Jean Langhorne (National Institute of Medical Research). DNA sequencing of these amplified regions was then completed to obtain the amino acid sequence for *P. chabaudi chabaudi* strain AS AMA1. The sequencing was done at the Wellcome Trust Centre for Human Genetics, Oxford University, and MWG Biotech (Ebensburg, Germany). The sequence of *P. chabaudi chabaudi* strain AS AMA1 differed from that of *P. chabaudi adami* (strain DS) by 34 aa (Supplemental Fig. 1). The vaccine construct encoded the ectodomain of *P. chabaudi chabaudi* strain AS AMA1 (aa 25–546) and included 4 aa substitutions to remove potential sites of N-linked glycosylation ([original amino acid position > new amino acid] S-136 > A, T-191 > A, S-233 > A, S-251 > A). The native parasite N-terminal signal sequence, transmembrane domain, and the C-terminal cytoplasmic domain were not included. The construct was codon optimized for expression in mice and synthesized by GeneArt (Regensburg, Germany). The tissue plasminogen activator leader sequence replaced the native AMA1 signal sequence as previously described (12). This construct was used to make recombinant AdHu5 and MVA by methods that were described previously (9). The vector control vaccines were AdHu5 with the transgene promoter and polyA tail, but no antigenic insert, and MVA expressing GFP (37). AdHu5 was chosen as a model adenovirus without intellectual property restrictions that is suitable for preclinical vaccine work. The immunogenicity and efficacy of AdHu5 vaccines can be readily matched by clinically applicable simian adenoviruses; we recently showed that the immunogenicity of AdHu5 and various simian adenoviruses is comparable in animal studies (11, 12, 15, 17) and that ChAd63 viruses are highly immunogenic and safe in both nonhuman primate studies (8) and in human clinical trials (13, 14).

Animals and immunizations

Five- to six-week-old female BALB/c (H-2^d) mice (John Radcliffe Hospital, Oxford, U.K. or Harlan, U.K.) were used, as stated, in all experiments. RAG 1/2 knockout mice were a kind gift from Dr. Nicholas Jones (Nuffield Department of Surgery, University of Oxford). The nude mice were obtained from Harlan. All procedures were performed according to the terms of the U.K. Animals (Scientific Procedures) Act Project License (PPL 30/2414) and Personal License (PIL 30/7792) and were approved by the University of Oxford Animal Care and Ethical Review Committee. The vaccines were diluted in endotoxin-free Dulbecco's PBS prior to immunization. Vaccines were administered intradermally (i.d.) bilaterally into the ears in a total volume of 50 μl for both recombinant adenovirus and MVA. The doses of recombinant adenovirus vaccines used were 5 × 10^{10} viral particles (vp), 1 × 10^{10} vp, or 1 × 10^9 vp; the dose of recombinant MVA vaccine used was always 1 × 10^7 PFU. The interval between the prime immunization with AdHu5-*P. chabaudi chabaudi* strain AS AMA1 and boosting with MVA-*P. chabaudi chabaudi* strain AS AMA1 was 8 wk in all experiments.

Total IgG ELISA

The Abs induced by vaccination were measured by ELISA, as previously described (9). Briefly, recombinant *P. chabaudi chabaudi* strain AS protein

was adsorbed to 96-well Nunc-Immuno Maxisorp plates at a concentration of 5 μg/ml in PBS. *P. chabaudi chabaudi* strain AS protein was a kind gift from Dr. Jean Langhorne. The *P. chabaudi chabaudi* strain AS parasite lysate preparation is described below and was coated at a concentration of 2 μg/ml in PBS. After blocking, the serum was incubated for 2 h, and the bound Abs were detected using alkaline phosphatase-conjugated goat anti-mouse IgG (whole molecule) (Sigma-Aldrich, Dorset, U.K.) diluted 1:5000. Serum Ab end point titers were taken as the *x*-axis intercept of the dilution curve at an absorbance value 3 SD greater than the OD_{405} for naive mouse serum (typical cut-off OD_{405} for positive sera = 0.15). Serum from naive mice was pooled and used as controls for all ELISAs.

Multiparameter flow cytometry

Cytokine secretion by PBMCs and splenocytes was assayed by intracellular cytokine staining (ICS). PBMCs and splenocytes were prepared, and the ICS assay was performed as previously described (7). Briefly, 100 μl cells were added to a 96-well U-bottom plate. Fifty microliters of 1 μg/ml brefeldin A (GolgiPlug; BD Biosciences) and 50 μl peptide diluted in complete medium were added to the test wells. Individual or pooled peptides (Peptide Protein Research, Hampshire, U.K.) are described in Tables I and II and were added at a final concentration of 1 μg/ml. In the control unstimulated wells, GolgiPlug and medium were added. Cells were incubated at 37°C 5% CO_2 for 5 h. After incubation, the cells were left at 4°C overnight. The next day, cells were surface stained for 30 min at 4°C with PerCP-Cy5.5–conjugated anti-mouse CD8α (clone 53-6.7) and Pacific Blue-labeled anti-mouse CD4 (clone LT34) diluted in PBS with 0.1% BSA at a dilution individually assessed by titration for each Ab. Cells were then permeabilized in 100 μl 1× Cytofix/Cytoperm solution (BD Biosciences) for 20 min at 4°C and then intracellularly stained for 30 min at 4°C with allophycocyanin-conjugated anti-mouse IFN-γ (clone XMG1.2), FITC-conjugated anti-mouse TNF-α (clone 145-2C11), and PE-conjugated anti-mouse IL-2 (clone JES6-5H4). After staining, cells were resuspended in 200 μl PBS containing 1% formalin. Samples were analyzed using an LSRII Flow Cytometer (BD Biosciences) and FlowJo v8.8 (Tree Star). The Boolean gate platform was used with individual gates to create response combinations. Pestle v1.6 and SPICE v5.0 software (38) were used to analyze the T cell-response profiles. Background responses in unstimulated control cells were subtracted from the peptide-stimulated response.

Parasites and blood-stage challenge

P. chabaudi chabaudi strain AS parasites were kindly provided by Dr. Jean Langhorne. Five days prior to challenge, a frozen aliquot of *P. chabaudi chabaudi* strain AS-infected blood was thawed and injected i.p. into a donor BALB/c mouse. On the day of challenge, the number of RBCs/μl of blood was counted (39), and the percentage of parasitemia was measured by counting a Giemsa-stained thin-blood smear. This was used to calculate the number of parasitized RBCs (pRBCs)/ml of blood. Blood from the donor mouse was diluted accordingly in PBS + 0.2% glucose supplemented with 10% naive mouse serum (Sigma-Aldrich) to give 1×10^7 pRBCs/ml, unless otherwise stated. Mice were injected with 100 μl this solution (1×10^6 pRBCs) i.v. via the tail vein. From day 4 post-challenge, the parasitemia was monitored daily by Giemsa-stained thin-blood smear, and the health status was monitored twice daily during acute parasitemia. *P. chabaudi chabaudi* strain AS nonlethal infection in naive wild-type BALB/c mice reaches a maximum parasitemia of 50–60% and is then controlled. *P. chabaudi adami* strain DS and strain DK parasites were kindly provided by Dr. Alison Creasey (Institute of Immunology and Infection Research, Edinburgh University, Edinburgh, U.K.). Challenges were performed as described for *P. chabaudi chabaudi* strain AS.

Blood-stage P. chabaudi chabaudi strain AS parasite lysate

Mice were injected with *P. chabaudi chabaudi* strain AS-infected pRBCs, and the parasitemia was monitored until it reached ∼20–30%. The mice were then sacrificed and bled by cardiac puncture into 10× heparin (final heparin concentration 30 U/ml blood), and the blood was pooled and stored on ice. The blood was centrifuged at 2500 rpm for 5 min, and the supernatant was removed carefully using a pipette. The pellet was then resuspended in 5 ml PBS and mixed by inverting the tube five or six times. A Plasmodipur filter (Euro-Diagnostika) was prepared with PBS, and the sample was passed through the filter using a 20-ml syringe. The original tube was washed with PBS and filtered twice. The cells were washed after filtration with 10 ml PBS and resuspended in 8 ml PBS + 0.06% saponin, mixed, and incubated at room temperature for 10 min. After the incubation, the sample was centrifuged at 2500 rpm for 5 min, and the pellet was washed twice in 5 ml PBS and resuspended in 1 ml PBS. This was then freeze-thawed three times to lyse the cells and centrifuged at 2500 rpm for

5 min before the supernatant was transferred to another tube. This was centrifuged at 12,000 rpm for 30 min to remove any remaining insoluble material. The protein concentration of the lysate was measured using a NanoDrop.

In vivo CD4⁺ T cell depletion

CD4⁺ T cells were depleted using anti-CD4 GK1.5 (rat IgG2a) mAb, as previously described (7). The mAb was purified using protein G affinity chromatography from hybridoma culture supernatants. Mice were injected i.p. with 200 μg mAb diluted in PBS on days −2, −1, and 0 (with respect to challenge on day 0), and the control mice were given normal rat polyclonal IgG (Sigma-Aldrich) purified in the same way. The degree of in vivo CD4⁺ T cell depletion was assessed by flow cytometry in the PBMCs of representative depleted and undepleted control mice, and it was shown to be >98%. A different anti-CD4 mAb clone (RM4.4) was used to stain CD4, to confirm that the CD4⁺ T cells were depleted (rather than the staining mAb binding being blocked by GK1.5) (Supplemental Fig. 2).

Adoptive transfer of CD4⁺ T cells

Splenocytes were prepared from immunized mice (as described in the text), and CD4⁺ T cells were isolated using the CD4⁺ T Cell Isolation Kit (MACS; Miltenyi Biotec) by depletion of non-CD4⁺ T cells (negative selection). Briefly, splenocytes were resuspended in 40 ml MACS buffer, and the cells were counted using a CASY counter (Schärfe Systems, Reutlingen, Germany). Cells were then centrifuged at $300 \times g$ for 10 min, and 40 μl MACS buffer/1×10^7 cells was added. Ten microliters/1×10^7 cells of biotin-conjugated Ab cocktail containing biotin-conjugated mAb against CD8α (Ly-2), CD45R (B220), DX5, CD11b (Mac-1), and Ter-119 was added to this, mixed, and incubated for 10 min at 4°C. After the incubation, 30 μl MACS buffer and 20 μl Anti-Biotin Microbeads/1×10^7 cells were added and incubated for 15 min at 4°C. Cells were then washed with buffer by adding 10× the labeling volume and centrifuged at $300 \times g$ for 10 min. The supernatant was discarded, and the cell pellet was resuspended in 500 μl buffer/1×10^8 total cells.

Magnetic separation of the cells was performed using a MACS separator and LS column (MACS; Miltenyi Biotec). Columns were attached to the magnets in the MACS separator and prepared by rinsing with 3 ml MACS buffer. The cell suspension was added to the column in units of 10 ml and allowed to pass through. The effluent was collected, which contained the unlabeled cells (i.e., the CD4⁺ T cell-enriched fraction). The columns were then washed four times with 3 ml MACS buffer, and the flow-through was collected into the same tube as the effluent. The cells were then spun down and resuspended in PBS, and the cell count was determined. After counting the cells, they were centrifuged at $300 \times g$ for 5 min, and the pellet was resuspended in a suitable volume of PBS for injection. A total of 9×10^7 CD4⁺ T cells was injected i.v. in a 200-μl volume/mouse 2 d before pRBC challenge.

Statistical analysis

Data were analyzed for statistical significance using GraphPad Prism v5 (GraphPad Software, San Diego, CA). The normality of the data set was determined using the Kolmogorov–Smirnov one-sample test. For nonparametric data, a Mann–Whitney U test was used to compare two groups. Parametric data were compared either using the t test (for comparing two groups) or one-way ANOVA (for comparing more than two groups). A post hoc Dunnett correction was used to compare test groups to one control group, whereas a Bonferroni correction was used when all of the groups were compared with each other. ELISA titers were logarithmically (log10) transformed to normalize the data and enable a more stringent parametric analysis. The area under the curve (AUC) was calculated to analyze the challenge data, and the different groups were compared by ANOVA. A *p* value ≤ 0.05 was considered significant.

Results

P. chabaudi chabaudi AS AMA1 sequence and vaccine design

The complete coding sequence of *P. chabaudi chabaudi* strain AS AMA1 was not available, so primers were designed against conserved regions by comparing sequences from related strains (40), and the sequence was determined (GenBank accession number JF690775, http://www.ncbi.nlm.nih.gov/nuccore/JF690775) (Supplemental Fig. 1). A vaccine construct (termed *P. chabaudi chabaudi* strain AS AMA1) was subsequently designed that contained the ectodomain of *P. chabaudi chabaudi* strain AS AMA1, with

four potential sites of N-linked glycosylation removed (described in *Materials and Methods*). The construct was codon optimized for expression in mice, synthesized, and used to generate recombinant AdHu5 and MVA vectors, as described in *Materials and Methods*.

Ab responses induced by AdHu5-MVA P. chabaudi chabaudi *strain AS AMA1 prime-boost vaccination*

BALB/c mice were immunized i.d. with 5×10^{10} vp of AdHu5-*P. chabaudi chabaudi* strain AS AMA1 and boosted 8 wk later i.d. with 1×10^7 PFU of MVA-*P. chabaudi chabaudi* strain AS AMA1. This 8-wk interval was shown to be important for both Ab and T cell responses when using these two vectors in a prime-boost vaccination regimen (9, 41). Serum was obtained 2 wk postprime (day 14), preboost (day 55), and 2 wk postboost (day 70). The total IgG response against the ectodomain of *P. chabaudi chabaudi* strain AS AMA1 was measured by ELISA. In agreement with other murine data for the AdHu5 vector, there were detectable AMA1-specific IgG responses 2 wk after the AdHu5 priming immunization, and these increased over time to become significantly higher at day 55. MVA administration on day 56 boosted the Ab level significantly, as measured on day 70 (Fig. 1).

T cell responses induced by AdHu5-MVA P. chabaudi chabaudi *strain AS AMA1 prime-boost vaccination*

A previous study mapped both immunodominant and cryptic epitopes within *P. chabaudi adami* AMA1 following immunization of BALB/c mice with rAg (32). The T cell responses induced against *P. chabaudi chabaudi* strain AS AMA1 by AdHu5-MVA immunization were measured in this study by ICS following restimulation of splenocytes with peptides corresponding to the previously reported CD4$^+$ T cell epitopes, as well as predicted CD8$^+$ T cell epitopes. Six peptide pools containing 15 mer peptides, overlapping by 10 aa, were tested. The peptides were divided into pools according to whether they were reported to contain CD4$^+$ T cell epitopes (32) or predicted CD8$^+$ T cell epitopes, as well as according to the position of the peptide within the Ag (Table I). Pool 1 contained 10 peptides (P7–P16) that included the known immunodominant CD4$^+$ T cell epitope. Pool 2 (P25 and P26), Pool 3 (P29 and P30), and Pool 4 (P74 and P75) each contained two peptides and were predicted to be H-2^d CD8$^+$ T cell epitopes from known H-2 class I-binding motifs. Pool 5 (P79 and P80) and Pool 6 (P84 and P85) also contained two peptides each, which were published by Good et al. (32) to be CD4$^+$ T cell immunodominant epitopes. Splenocytes from BALB/c mice, har-
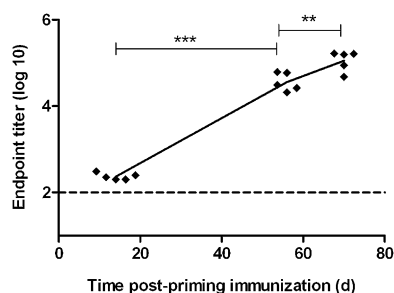
Table I. *P. chabaudi chabaudi* strain AS AMA1 peptides tested by ICS

Pool	Peptide #	Amino Acid Sequence	Amino Acid Position	CD4 or CD8
Pool 1	P7	LINPWEKFMEKYDIE	51–65	CD4
	P8	EKFMEKYDIEKVHGS	56–70	
	P9	KYDIEKVHGSGIRVD	61–75	
	P10	KVHGSGIRVDLGEDA	66–80	
	P11	GIRVDLGEDARVENQ	71–85	
	P12	LGEDARVENQDYRIP	76–90	
	P13	RVENQDYRIPSGKCP	81–95	
	P14	DYRIPSGKCPVMGKG	86–100	
	P15	SGKCPVMGKGITIQN	91–105	
	P16	VMGKGITIQNSKVSF	96–110	
Pool 2	P25	ANLKLMYKDHKEILA	141–155	CD8
	P26	MYKDHKEILALNDMS	146–160	
Pool 3	P29	LCAKHASFYVPGTNV	161–175	CD8
	P30	ASFYVPGTNVNTAYR	166–180	
Pool 4	P74	SFPCDIYKKKIAEEI	386–400	CD8
	P75	IYKKKIAEEIKVMNV	391–405	
Pool 5	P79	GNGTIQFPRIFISDD	411–425	CD4
	P80	QFPRIFISDDKESLK	416–430	
Pool 6	P85	SSCNFFVCNCVEKRQ	441–455	CD4
	P86	FVCNCVEKRQFISEN	446–460	

The table shows the six peptide pools tested by ICS, as well as the amino acid sequence of each peptide. The far right column indicates whether the peptide pools contained published CD4$^+$ T cell epitopes (32) or predicted CD8$^+$ T cell epitopes (using the epitope prediction section of the SYFPEITH Web site; http://www.syfpeithi.de).

vested 2 wk after AdHu5-MVA *P. chabaudi chabaudi* strain AS AMA1 immunization (day 70), were restimulated with the peptide pools for 5 h, surface stained for CD4 and CD8, and then intracellularly stained for IFN-γ, TNF-α, and IL-2. Pools 1 and 5 were identified as containing peptides that were recognized by CD4$^+$ T cells, leading to the production of IFN-γ (Fig. 2A). Similarly, TNF-α$^+$ and IL-2$^+$ CD4$^+$ T cell responses were also measured in cells restimulated with Pool 1 and Pool 5 (data not shown). There were no CD8$^+$ IFN-γ$^+$ T cell responses detected to any of the peptide pools tested (Fig. 2B). The individual epitopes within the responding peptide pools were then identified in a repeat experiment. This showed that the CD4$^+$ IFN-γ$^+$ T cell responses in BALB/c mice against the ectodomain of *P. chabaudi chabaudi* strain AS AMA1 were against epitopes present within two peptides: P16 (within Pool 1) and P79 (within Pool 5) (Fig. 2C–E). These cells produced all three cytokines assayed, but the percentages of IFN-γ– (Fig. 2C) and TNF-α–secreting cells (Fig. 2D) tended to be slightly higher than the percentages of cells secreting IL-2 (Fig. 2E).

Two CD4$^+$ T cell epitopes had now been identified, and these were in agreement with those reported to be induced following immunization with recombinant AMA1 protein in adjuvant (32). In this study using a viral-vectored vaccination regimen, it remained possible that T cell responses to other epitopes were induced in addition to those identified after protein immunization. To confirm whether any other T cell responses were induced against the AMA1 Ag, 15 mer peptides overlapping by 10 aa were synthesized that covered the entire ectodomain of *P. chabaudi chabaudi* strain AS AMA1 contained within the vaccine insert (Supplemental Table I). Splenocytes, isolated as before, were subsequently restimulated with seven overlapping peptide pools (10 peptides in each pool) or no peptide (Unstim) and assayed by ICS. The CD4$^+$ T cell epitopes P16 and P79, identified in the previous set of experiments (Fig. 2C), were included as positive controls. There were no further CD4$^+$ IFN-γ$^+$ T cell responses identified in any of the peptide pools (Fig. 3A); however, a very weak CD8$^+$ IFN-γ$^+$ T cell response was measured in three of five mice in Pool 11 (Fig. 3B).

FIGURE 1. Ab responses induced by AdHu5-MVA *P. chabaudi chabaudi* strain AS AMA1 prime-boost vaccination. BALB/c mice (*n* = 5) were primed with 5×10^{10} vp of AdHu5-*P. chabaudi chabaudi* strain AS AMA1 and boosted 8 wk later with 1×10^7 PFU of MVA-*P. chabaudi chabaudi* strain AS AMA1. The AMA1-specific total IgG response against recombinant *P. chabaudi chabaudi* strain AS AMA1 ectodomain was measured by ELISA in the serum at days 14 (postprime), 55 (preboost), and 70 (postboost). Each point indicates the response from an individual mouse, and the line links the mean. **$p \leq 0.01$, ***$p \leq 0.001$, paired *t* test.

FIGURE 2. Identification of splenic T cell responses to AMA1 following AdHu5-MVA *P. chabaudi chabaudi* strain AS AMA1 immunization. Mice were immunized with the same regimen as in Fig. 1. Two weeks postboost (day 70), splenocytes were isolated and restimulated with pools of overlapping peptides (P1–P6, Table I) or no peptide (Unstim). Cells were surface stained for CD4 and CD8, intracellularly stained for IFN-γ, and assessed by flow cytometry to determine the percentage of responding cells per total CD4^{+} (**A**) or CD8^{+} (**B**) T cell subset. The bars represent the mean response ± SEM (*n* = 5). In a repeat experiment, splenocytes were restimulated with individual peptides from Pool 1 (P7 to P16) or Pool 5 (P79 and P80) or no peptide (Unstim). Cells were surface stained for CD4, intracellularly stained for IFN-γ (**C**), TNF-α (**D**), and IL-2 (**E**), and assessed by flow cytometry to determine the percentage of responding cells/total CD4^{+} T cell subset. The bars represent the mean response ± SEM (*n* = 5).
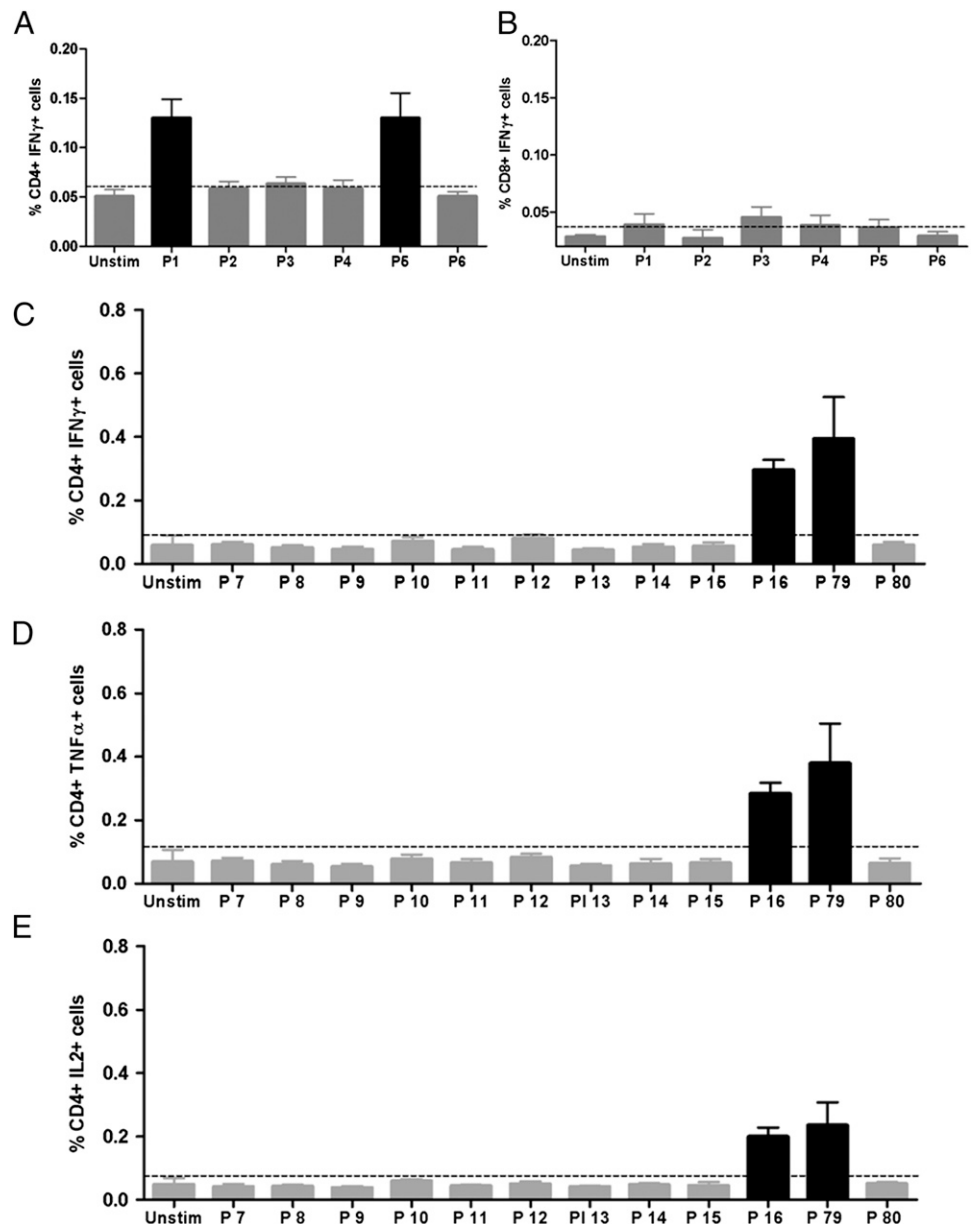
The functionality of the P16- and P79-specific splenic CD4^{+} T cells was also analyzed after the AdHu5-*P. chabaudi chabaudi* strain AS AMA1 prime (day 14) and the MVA-*P. chabaudi chabaudi* strain AS AMA1 boost (day 70) (Fig. 4). Triple-positive cells were defined as cells that simultaneously produce the three cytokines assayed (IFN-γ, TNF-α, and IL-2) (42), double-positive cells simultaneously produce any two of the three cytokines, and single-positive cells produce only one cytokine. For the P16 epitope, the number of triple-positive cells producing IFN-γ, TNF-α, and IL-2 did not change significantly after the boost (Fig. 4A). However, there was a significant increase (~2–5-fold) in the number of double-positive cells producing IFN-γ and IL-2 or IFN-γ and TNF-α (*p* = 0.02 and *p* = 0.004, respectively, Mann–Whitney *U* test). Cells producing only TNF-α were not detectable, and there was no significant increase in the number of cells producing only IFN-γ or IL-2 after the MVA boost. For the P79 epitope, the functionality profile of the CD4^{+} T cells was very similar to that of P16 (Fig. 4B). Overall, these data showed an increased frequency of CD4^{+} T cells producing IFN-γ and IL-2 or IFN-γ and TNF-α after the booster immunization, in conjunction with an increase in the overall magnitude of the Ag-specific response.

Protective efficacy of AdHu5-MVA P. chabaudi chabaudi *strain AS AMA1 vaccination against blood-stage challenge*

The protective efficacy of the AdHu5-MVA *P. chabaudi chabaudi* strain AS AMA1 prime-boost vaccination regimen was assessed by blood-stage challenge with *P. chabaudi chabaudi* strain AS parasites. Immunized mice were challenged 2 wk postboost (day 70) i.v. with 10[5] *P. chabaudi chabaudi* strain AS pRBCs. Naive unimmunized control BALB/c mice were challenged at the same time. Parasitemia was monitored from day 4 postchallenge by Giemsa-stained thin-blood smears, and the results are expressed as the percentage of infected RBCs (Fig. 5). Given that *P. chabaudi chabaudi* strain AS infection in naive BALB/c mice is nonlethal, protective efficacy was assessed by comparing parasitemia between the groups. Significantly lower mean parasitemia was observed in the AdHu5-MVA *P. chabaudi chabaudi* strain AS AMA1-vaccinated mice in comparison with the naive controls from the time of patency (day 4) until day 7. At the time of peak
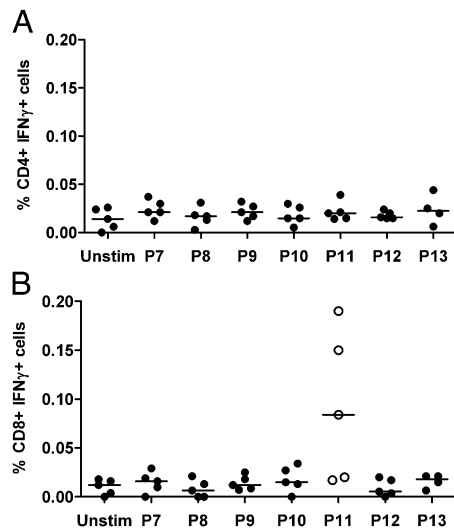
FIGURE 3. T cell epitope mapping within the entire ectodomain of *P. chabaudi chabaudi* strain AS AMA1. Mice were immunized with the same regimen as in Fig. 1. Two weeks postboost (day 70), splenocytes were restimulated for 5 h with seven overlapping peptide pools containing 10 peptides each (Pool 7–13, Supplemental Table I) or no peptide (Unstim). The cells were then surface stained for CD4 or CD8 and intracellularly for IFN-γ. The figure shows the percentage of CD4⁺ IFN-γ⁺ cells (**A**) or CD8⁺ IFN-γ⁺ cells (**B**). Responses from individual mice are shown, and the lines represent the median.

parasitemia (day 7), the vaccinated mice had significantly lower levels of infection (geomean ± SD = 24.6 ± 2.6% versus 43.4 ± 5.6% in the naive controls, $p = 0.002$). These data confirmed that the vaccine could lead to significant control of peak parasitemia in these mice, although the rate of parasite clearance following this was comparable between the vaccinees and controls. It was confirmed in a repeat experiment that this control of peak parasitemia occurs following Ag-specific immunization. The same result was observed following challenge of mice immunized with nonrecombinant/control AdHu5 and MVA vaccines (Supplemental Fig. 3A).

In vivo depletion of CD4⁺ T cells prior to challenge results in a loss of vaccine-induced protection

Previous work analyzing protective immune mechanisms in the *P. chabaudi adami* model demonstrated a role for Abs either induced by active immunization with recombinant AMA1 or passively transferred from the sera of immunized rabbits (40, 43), as well as for CD4⁺ T cells acting independently of, or in concert with, AMA1-specific Abs (31, 32). Thus, the contribution of CD4⁺ T cells in vaccine-induced protection in this *P. chabaudi chabaudi* strain AS model was initially assessed by in vivo CD4⁺ T cell depletion prior to blood-stage challenge. The anti-mouse CD4 GK1.5 (rat IgG2a) mAb was reported to deplete CD4⁺ T cells for up to 10 d, after which they are replenished to ~50% of the original level by 4 wk (44). Two groups of mice were immunized as before with the AdHu5-MVA *P. chabaudi chabaudi* strain AS AMA1 vaccine regimen. CD4⁺ T cells were depleted in one group of the vaccinated mice, as well as in one group of naive controls, prior to i.v. challenge with 10^6 *P. chabaudi chabaudi* strain AS pRBCs. The undepleted vaccinated and naive mice were administered the same amount of normal rat polyclonal IgG.

In this experiment, a similar degree of protective efficacy was observed for the AdHu5-MVA *P. chabaudi chabaudi* strain AS AMA1 vaccination regimen in undepleted mice, even though the challenge dose was increased to 10^6 pRBCs (Fig. 6A) compared with a challenge with 10^5 pRBCs in the previous experiment (Fig.

5). Mean peak parasitemia was again significantly reduced in the vaccinated mice in comparison with the naive controls at days 6 and 7 postchallenge (Fig. 6A). However, CD4⁺ T cell depletion resulted in the loss of vaccine efficacy in immunized mice, as reflected by increased peak parasitemias on days 6–7 that were comparable to those of undepleted naive controls (Fig. 6B), thus confirming an important contributory role for vaccine-induced CD4⁺ T cells to protection in this model. Interestingly, the vaccinated depleted mice also failed to clear the parasites as early as did the nondepleted mice, and a second wave of parasitemia was observed that peaked on day 13. An almost identical second wave was also observed in the naive depleted animals; overall they fared the worst, demonstrating a chronic patent parasitemia at 30 d postinfection (Fig. 6C). Also, in agreement with a previous report (31), the naive CD4⁺ T cell-depleted mice suffered the highest peak parasitemias on days 6–7 (Fig. 6D).

Role of P. chabaudi chabaudi *strain AS AMA1-specific and whole-parasite Abs in clearance*

Unlike the control of peak parasitemia, parasite clearance in the *P. chabaudi* model is attributed to B cells and Abs (27, 45). Thus, the faster rate of parasite clearance observed in the depleted vaccinated mice in comparison with naive depleted controls (Fig. 6C) could be due to the presence of vaccine-induced AMA1-specific Abs in the vaccinated mice that are able to control and clear parasites in the later stage of infection. Therefore, serum total IgG Ab titers against recombinant *P. chabaudi chabaudi* strain AS AMA1 protein and whole-parasite lysate were measured by ELISA 1 mo postchallenge (Fig. 7A). In agreement with the previously reported protein-vaccine study (31), there was no difference in *P. chabaudi chabaudi* strain AS AMA1-specific Ab titers in the vaccinated depleted versus nondepleted mice. A de novo *P. chabaudi chabaudi* strain AS AMA1-specific Ab response was detected in the non-CD4⁺ T cell-depleted naive control mice, but the titers were significantly lower than those seen in the vaccinated mice. There was no detectable *P. chabaudi chabaudi* strain AS AMA1-specific Ab response in the naive-depleted mice, suggesting that CD4⁺ T cell help is necessary for de novo *P. chabaudi chabaudi* strain AS AMA1 Ab production from B cells during infection.

Interestingly, the response to the whole *P. chabaudi chabaudi* strain AS parasite lysate was similar in the nondepleted vaccinated and naive groups, whereas there was a significantly lower Ab response to the whole parasite postchallenge in the CD4⁺ T cell depleted groups compared with the two nondepleted groups (Fig. 7B). Given that the naive CD4⁺ T cell-depleted mice were still parasitemic 1 mo postchallenge (Fig. 7C), it is interesting to note that these mice possessed no *P. chabaudi chabaudi* strain AS AMA1-specific Abs but had similar parasite lysate-specific Ab levels compared with the vaccinated depleted mice (who cleared the infection faster). However, both the vaccinated and the naive nondepleted mice cleared their parasites at the same time (Fig. 6A), although the naive mice possessed significantly lower levels of *P. chabaudi chabaudi* strain AS AMA1-specific Abs (Fig. 7A). Taken together, these data suggest that both *P. chabaudi chabaudi* strain AS AMA1-specific Abs and Abs to other parasite Ags are able to contribute to parasite clearance.

Adoptive transfer of CD4⁺ T cells from vaccinated mice to naive and immunocompromised mice

To further assess the contribution of vaccine-induced CD4⁺ T cells and Abs to the initial control of blood-stage parasite densities, a number of adoptive-transfer studies was undertaken. BALB/c mice were immunized exactly as before, and the spleen and serum were harvested from each mouse 2 wk after the MVA boost.
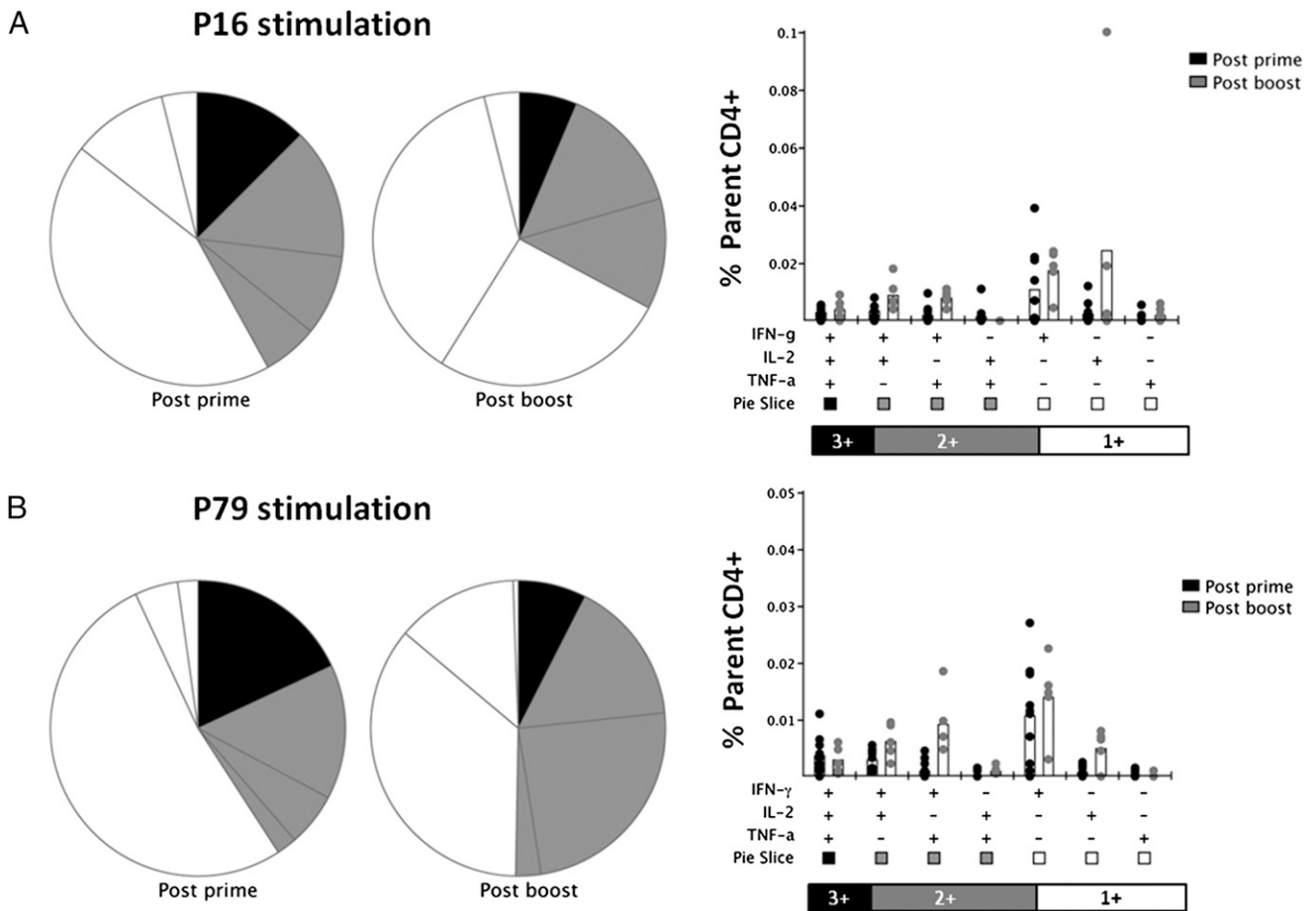
A P16 stimulation

B P79 stimulation

FIGURE 4. Multifunctionality of P16- and P79-specific CD4$^+$ T cells. Mice were immunized with the same regimen as described in Fig. 1. Two weeks postprime with AdHu5-*P. chabaudi chabaudi* strain AS AMA1 (day 14) and 2 wk postboost with MVA-*P. chabaudi chabaudi* strain AS AMA1 (day 70), splenocytes were restimulated with the P16 and P79 peptide or no peptide (Unstim) for 5 h. Cells were surface stained for CD4, intracellularly stained for IFN-γ, TNF-α, and IL-2, and assessed by flow cytometry to determine the percentage of responding cells/total CD4$^+$ T cell subset. Total responses of each cytokine to P16 (**A**) and P79 (**B**) are shown at each time point. The multifunctionality or "quality" of CD4$^+$ T cells was analyzed using SPICE software.

Mice were either immunized with AdHu5-MVA vectors encoding *P. chabaudi chabaudi* strain AS AMA1 or with an identical regimen using vector controls expressing no rAg. These vector controls did not express *P. chabaudi chabaudi* strain AS AMA1, thus enabling an assessment of the protective role of *P. chabaudi chabaudi* strain AS AMA1-specific CD4$^+$ T cells and confirming that any protective effect observed was not due to viral vector immunization per se. Splenic CD4$^+$ T cells from the vaccinated mice were isolated by negative selection (as described in *Materials and Methods*), and these or pooled sera were transferred into naive BALB/c mice (Fig. 8A–C). All mice were subsequently challenged with 10^6 *P. chabaudi chabaudi* strain AS pRBCs.

In agreement with the previous result (Fig. 6A), there was a significantly lower parasitemia (AUC analysis, $p = 0.008$) in the AdHu5-MVA *P. chabaudi chabaudi* strain AS AMA1-vaccinated control group in comparison with naive controls (Fig. 8A). This effect was mirrored in the naive wild-type mice that received the CD4$^+$ T cell transfer from vaccinated mice ($p = 0.008$, AUC versus naive controls). Moreover, although the mice that received the CD4$^+$ T cells from the Ad_M control-immunized controls showed transiently lower parasitemias than the naive controls on days 4 and 5, there was subsequently no significant difference in the AUC analysis ($p = 0.69$), unlike that observed in the mice receiving CD4$^+$ T cells from *P. chabaudi chabaudi* strain AS AMA1-immunized mice (Fig. 8A, 8B). These data confirm that vaccine-induced *P. chabaudi chabaudi* strain AS AMA1-specific CD4$^+$ T cells are an important contributing factor to the control of initial peak parasitemia in this model.
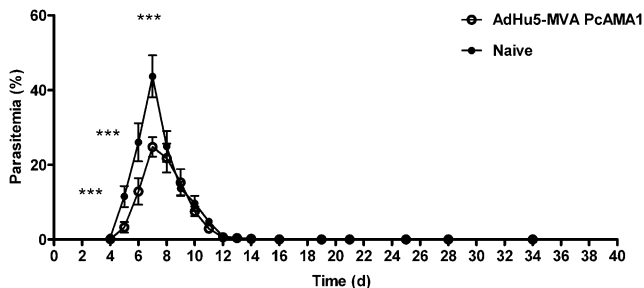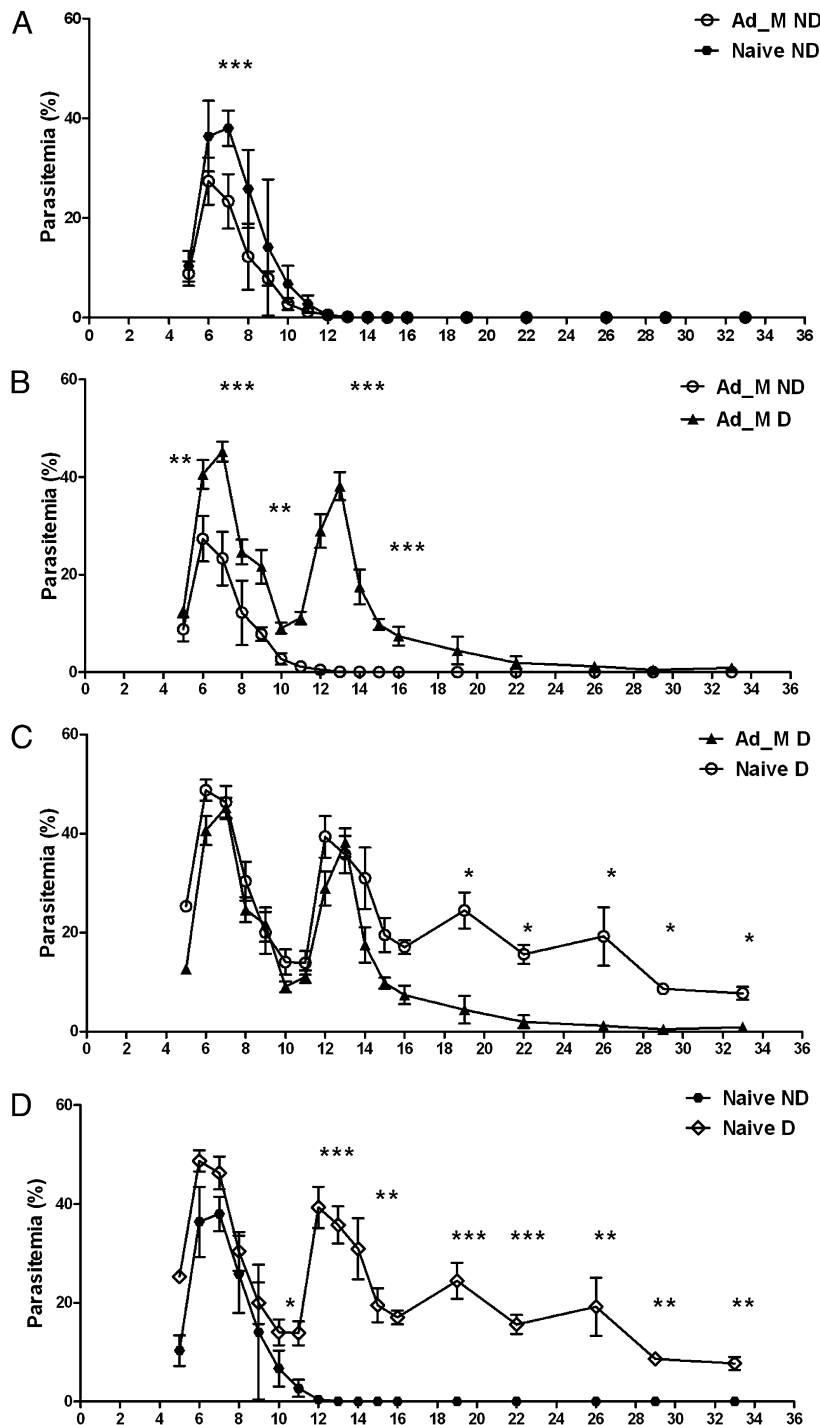

FIGURE 5. Efficacy of AdHu5-MVA *P. chabaudi chabaudi* strain AS AMA1 immunization against blood-stage challenge. BALB/c mice ($n = 6$) were vaccinated with 5×10^{10} vp of AdHu5-*P. chabaudi chabaudi* strain AS AMA1 and boosted 8 wk later with 1×10^7 PFU of MVA-*P. chabaudi chabaudi* strain AS AMA1. Two weeks after the MVA boost (day 70), these mice and six naive unvaccinated controls were challenged i.v. with 10^5 nonlethal *P. chabaudi chabaudi* strain AS pRBCs. Parasitemia was monitored daily from day 4 by Giemsa-stained thin-blood smears, and the results are expressed as the percentage of infected RBCs. The difference in parasitemia between the two groups was taken as the measure of vaccine efficacy. The mean percentage parasitemia ± SEM are shown. ***$p \leq$ 0.001, Mann–Whitney U test.

FIGURE 6. Effect of in vivo CD4$^+$ T cell depletion on vaccine efficacy. Two groups of BALB/c mice (*n* = 6/group) were vaccinated with 5 × 10^{10} vp of AdHu5-*P. chabaudi chabaudi* strain AS AMA1 and boosted 8 wk later with 1 × 10^7 PFU of MVA-*P. chabaudi chabaudi* strain AS AMA1. These mice and two groups of naive controls were challenged i.v. 14 d postboost with 10^6 pRBCs. One group each of vaccinated and naive mice were depleted of CD4$^+$ T cells, as described in *Materials and Methods*. Parasitemia was monitored daily by Giemsa-stained thin-blood smears, and the results are expressed as the percentage of infected RBCs (mean ± SEM). The difference in parasitemia between the groups was taken as the measure of vaccine efficacy. (**A**) Vaccinated nondepleted (Ad_M ND) and naive nondepleted (Naive ND) mice. (**B**) Vaccinated depleted (Ad_M D) and nondepleted (Ad_M ND) mice. (**C**) Vaccinated depleted (Ad_M D) and naive depleted (Naive D) mice. (**D**) Naive depleted (Naive D) and nondepleted (Naive ND) mice. *p ≤ 0.05, **p ≤ 0.01, ***p ≤ 0.001, Mann–Whitney *U* test.

Interestingly, serum transfers into normal naive BALB/c mice from AMA1- or control vaccinated mice showed a result similar to that for CD4$^+$ T cell transfer (Fig. 8C). The mice receiving serum from mice vaccinated with *P. chabaudi chabaudi* strain AS AMA1 had significantly lower initial parasite densities in comparison with naive controls (AUC, *p* = 0.01). The serum transfer from vector control-immunized mice led to no difference in parasitemia compared with the naive mice (AUC not calculated because one of the mice died on day 9 postchallenge). Taken together, these data suggest that both *P. chabaudi chabaudi* strain AS AMA1-specific CD4$^+$ T cells and Abs can contribute to the control of initial parasitemia in immunocompetent recipients.

CD4$^+$ T cell-transfer studies were also performed using athymic nude mice (BALB/c *nu/nu*), which lack T cells, and RAG1/2

knockout mice (BALB/c RAG1/2$^{-/-}$), which lack T and B cells. Previous studies showed that nude mice infected with *P. chabaudi chabaudi* strain AS develop a chronic parasitemia and exhibit high mortality (33, 46), with a similarly poor outcome in RAG2$^{-/-}$ knockout mice, many of which succumb within the first 15 d of infection (31, 33). In comparison with previous reports for the lethal challenge of nude mice that were not reconstituted (31, 33), the transfer of CD4$^+$ T cells from *P. chabaudi chabaudi* strain AS AMA1-immunized mice was sufficient to control the initial peak parasitemias, albeit at a higher level than that seen when naive normal mice were recipients (Fig. 8D). A similar result was obtained in the RAG1/2 knockout mice, and both immunocompromised strains showed comparable parasite densities up to day 11, followed by a second smaller wave of parasitemia peaking on day
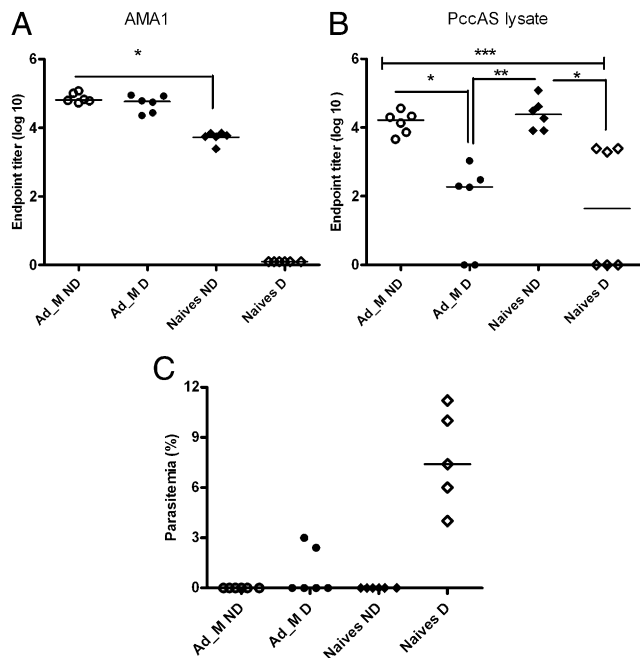
FIGURE 7. *P. chabaudi chabaudi* strain AS AMA1- and parasite-specific Ab responses postchallenge. Total IgG serum Ab levels in the mice shown in Fig. 6 were analyzed by ELISA 1 mo postchallenge (day 33). Individual responses plus the median are shown for *P. chabaudi chabaudi* strain AS AMA1 ectodomain (**A**) and whole *P. chabaudi chabaudi* strain AS parasite lysate (**B**). Significant differences in Ab levels between the different groups are indicated. (**C**) The corresponding individual and median percentage of parasitemia on day 33. *$p \leq 0.05$, **$p \leq 0.01$, ***$p \leq 0.001$, ANOVA.

13, an observation previously attributed to transfer of suboptimal CD4$^+$ T cell numbers (46). However, only two of five RAG1/2 knockout mice ultimately survived in comparison with four of five nude mice and, in agreement with similar studies using both naive wild-type or transgenic CD4$^+$ T cells specific for MSP1$_{33}$ (33), the RAG knockout mice that survived did not clear the infection, whereas the surviving nude mice cleared the parasites by day 30. Given that nude mice possess B cells, unlike RAG knockout mice, the trend for better survival and parasite clearance is consistent with reports detailing the importance of B cells with regard to these two outcomes.

T cell response to heterologous peptides from other P. chabaudi *strains*

Sequence polymorphism has remained a significant obstacle to the development of Ab-inducing AMA1 protein subunit vaccines (3, 47). Ab responses induced against AMA1 are allele specific, and vaccination with one allele does not confer cross-strain protection: an effect clearly shown in assays of *P. falciparum* in vitro growth inhibition (48), as well as homologous versus heterologous strain challenge studies in mice following *P. chabaudi* AMA1 protein immunization (41). Having shown a protective contribution of vaccine-induced CD4$^+$ T cells, it was of interest to ascertain whether the induction of cellular immunity by the AdHu5-MVA vaccines could help to improve cross-strain protection.

Initially, the amino acid sequences of the two CD4$^+$ T cell epitopes, P16 and P79, were compared across various parasite strains: *P. chabaudi chabaudi* AS (vaccine strain), *P. chabaudi adami* 556/DK, *P. chabaudi adami* CB, and *P. chabaudi adami* DS. As previously reported for the immunodominant epitopes mapped in *P. chabaudi adami* DS following AMA1 protein im-

munization, neither the P16 nor the P79 sequences were highly conserved between these four *P. chabaudi* strains. P16 was conserved in all but *P. chabaudi adami* DS, whereas the sequence of P79 was different from the vaccine *P. chabaudi chabaudi* AS strain in all of the other three strains compared (Table II). The heterologous peptides P16B and P79B, encoding the alternative sequences, were used to restimulate splenocytes from immunized mice, as described before; as expected, there was no detectable response to these heterologous peptides (Fig. 9). Given that the P16 epitope is partially conserved, we sought to ascertain whether the response to this epitope alone (in the absence of strain-specific Abs) could lead to initial control of parasite densities following heterologous parasite challenge. However, there was no protection observed in this experiment against the heterologous strain *P. chabaudi adami* DK (Supplemental Fig. 3B).

Discussion

The AMA1 Ag remains a leading candidate Ag for inclusion in a subunit vaccine against blood-stage *P. falciparum* malaria. However, despite extensive efforts, candidate protein-in-adjuvant vaccines tested for efficacy in phase IIa/b trials have shown minimal or strain-specific efficacy (47, 49). In this study, we characterized in detail the immunogenicity and protective efficacy of a prime-boost vaccination regimen using an alternative human-compatible vaccine-delivery platform encoding the *P. chabaudi chabaudi* strain AS AMA1 Ag. The *P. chabaudi* rodent malaria model remains a key example of how cellular immunity, acting independently of Abs, can significantly contribute to immune control of ascending early-phase blood-stage parasitemia, and these data confirm that viral-vectored vaccines are capable of inducing CD4$^+$ T cell responses that can fulfill that role. To develop viral vectors encoding *P. chabaudi chabaudi* strain AS AMA1, the complete sequence of the Ag was obtained from sequencing a PCR fragment amplified from parasite genomic DNA. The entire ectodomain was subsequently included in the viral vaccine transgene insert, given that this was previously shown in this model to induce protective immune responses (31, 40). The AdHu5-*P. chabaudi chabaudi* strain AS AMA1 vaccine primed a detectable Ab response that increased over time and that was significantly boosted after the administration of MVA-*P. chabaudi chabaudi* strain AS AMA1. These data are in accordance with previous findings in the *P. yoelii* model using viral vectors expressing MSP1$_{42}$ or the circumsporozoite protein, in which an 8-wk interval between prime and boost was shown to induce high-titer Abs, as well as strong T cell responses (9, 37). The kinetics of the Ab response are similar to those seen following vaccination with AdHu5 expressing other Ags, such as Ebola virus glycoprotein (50) or OVA (51), in which the Ab response increased by a similar order of magnitude over time and then reached a plateau by 6 wk postvaccination.

Analysis of the T cell responses in the spleen of immunized BALB/c mice, using overlapping peptides spanning the entire length of the *P. chabaudi chabaudi* strain AS AMA1 Ag, revealed two CD4$^+$ T cell epitopes. These peptides (P16 and P79) corresponded to those that were previously described by Amante et al. (32) after immunization with recombinant AMA1 protein-in-adjuvant. The investigators referred to these as immunodominant epitopes, in contrast to cryptic epitopes, which only elicit detectable responses in vitro following immunization of mice with the relevant peptide(s). Thus, the data generated in this study, using viral-vectored vaccines, are in agreement with their previous observations, with the exception of a very weak CD8$^+$ T cell response, which was also detected in some mice, to one of the
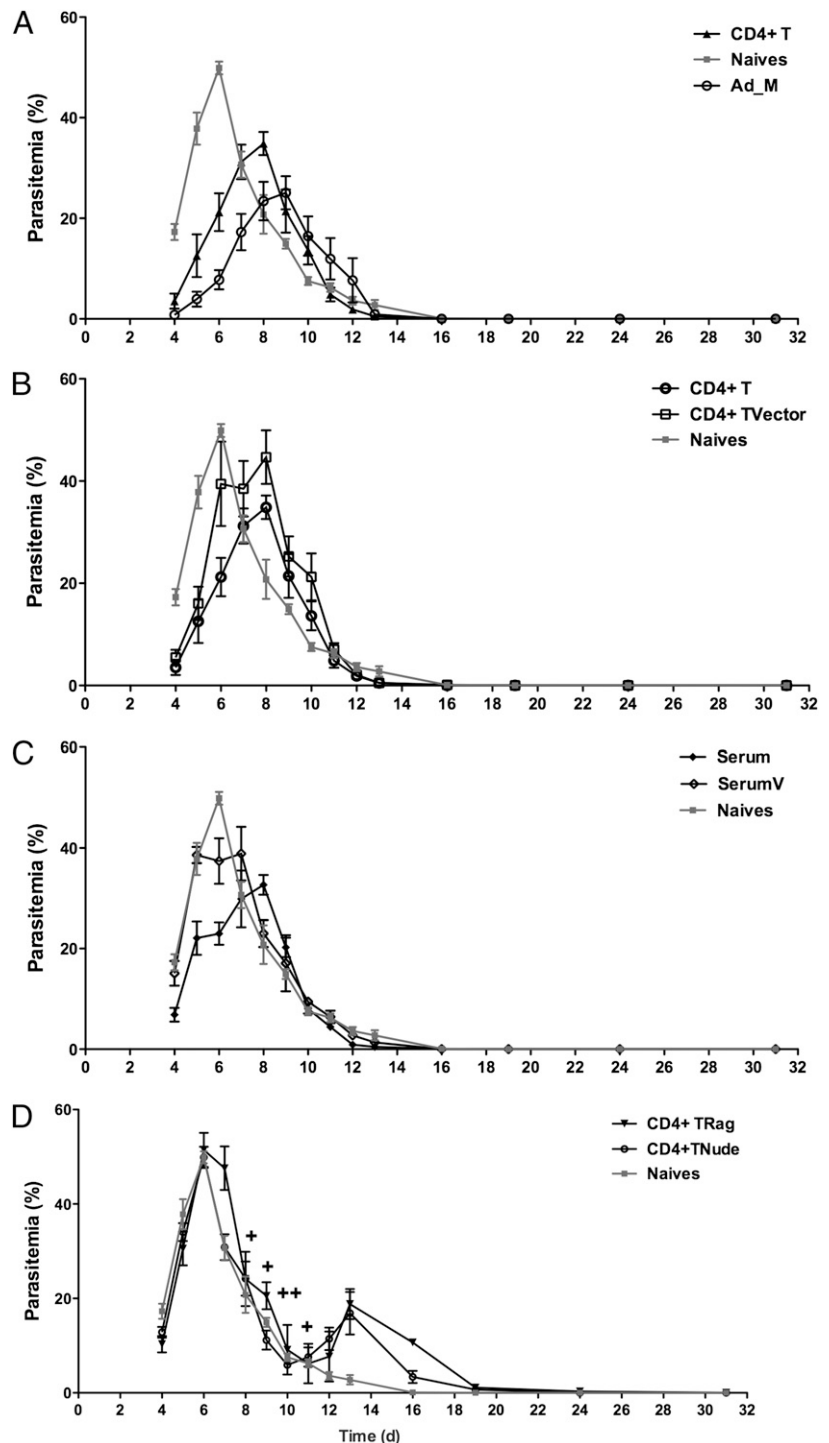
FIGURE 8. Adoptive transfer of CD4^{+} T cells and serum from vaccinated mice into normal and immunocompromised mice. BALB/c mice were immunized as before with AdHu5-MVA *P. chabaudi chabaudi* strain AS AMA1. Two weeks after the MVA boost, spleens were harvested and pooled, and the CD4^{+} T cells were isolated as described in *Materials and Methods*. A total of 9×10^7 CD4^{+} T cells from vaccinated mice were injected i.v. into naive wild-type mice (CD4^{+} T), RAG1/2[−/−] mice (CD4^{+} TRag), or BALB/c athymic nude (*nu/nu*) mice (CD4^{+} TNude). CD4^{+} T cells from vector control-immunized mice were also isolated and transferred into naive wild-type mice (CD4^{+} TVector) in the same manner. Serum was also harvested from each vaccinated and vector control mouse, pooled, and transferred into two groups of naive wild-type mice (labeled as Serum and SerumV, respectively). Five hundred microliters of serum was injected i.p. on days −1 and 0 (total 1 ml into each mouse), with respect to challenge on day 0. A group of naive wild-type mice and vaccinated (Ad_M) control mice were also included (*n* = 5 mice/group, except for the serum-transfer groups, where *n* = 4 mice/group). All mice were then challenged with 10^6 *P. chabaudi chabaudi* strain AS pRBCs and monitored as previously described. In the CD4^{+} TRag group, three mice died (one on each of days 8, 9, and 11; denoted by +); in the CD4^{+} TNude group, one mouse died (on day 10; denoted by ++). (**A**–**D**) Comparisons among the various groups and the mean group percentage of parasitemia ± SEM over time.

peptide pools tested. Interestingly, unlike the results previously seen with *P. yoelii* MSP1$_{33}$ Ag in BALB/c mice (7, 11, 52), no responses were measured to those peptides predicted to contain CD8^{+} T cell epitopes by the H-2[d] class I epitope motif analysis.

Similar to other studies using the AdHu5-MVA prime-boost regimen in mice (10, 42), vaccination induced multifunctional T cell responses, whereby cells simultaneously produce various combinations of cytokines (such as IFN-γ, TNF-α, and IL-2) following restimulation in vitro. It was shown that the frequency of CD4^{+} T cells producing all three of these cytokines correlates with protection against *Leishmania major* in mice (42), but this has not been investigated in the context of a mouse model of

blood-stage malaria, in which CD4^{+} T cell responses are known to be critical for protection. In the analysis described in this article, it was shown that, in some cases, the multifunctional profile of the AMA1-specific CD4^{+} T cells differed between those cells measured 14 d after the AdHu5 prime and those measured 14 d after the MVA boost. Because efficacy was only assessed in this study after AdHu5-MVA *P. chabaudi chabaudi* strain AS AMA1 immunization, and not following a single administration of AdHu5-*P. chabaudi chabaudi* strain AS AMA1, it is not possible to conclude whether these qualitative differences would translate into altered levels of vaccine efficacy. This assessment would also be confounded by the fact that the overall magnitudes of both the

Table II. Comparison of the peptide sequences containing the CD4$^+$ T cell epitopes identified in AMA1 across various strains of *P. chabaudi*

Peptide	Parasite Strain	Sequence	Vaccine Strain Homology
P16	*P. chabaudi chabaudi* AS	VMGKGITIQNSKVSF	Yes
P16	*P. chabaudi adami* 556/DK	VMGKGITIQNSKVSF	Yes
P16	*P. chabaudi adami* CB	VMGKGITIQNSKVSF	Yes
P16B	*P. chabaudi adami* DS	VMGKGITIQ**KSTK**SF	No
P79	*P. chabaudi chabaudi* AS	GNGTIQFPRIFISDD	Yes
P79B	*P. chabaudi adami* 556/DK	GN**DTIKF**PRIFISDD	No
P79B	*P. chabaudi adami* CB	GN**DTIKF**PRIFISDD	No
P79B	*P. chabaudi adami* DS	GN**DTIKF**PRIFISDD	No

Sequence comparison across various *P. chabaudi* strains for the two CD4$^+$ T cell epitopes identified in *P. chabaudi chabaudi* strain AS AMA1. The P16 and P79 peptides represent the amino acid sequence in the *P. chabaudi chabaudi* strain AS AMA1 vaccine. P16B and P79B represent peptides encoding the variant sequences identified in the heterologous strains. The amino acids shown in bold-type differ between the homologous and heterologous strains.

T cell and Ab responses are lower after a single AdHu5 immunization. In fact, few model systems provide the ability to assess the protective consequences of altered T cell "quality" in the context of constant overall quantity. This probably reflects the fact that T cell multifunctionality measured in vitro more likely represents a snapshot of the continuum of T cell phenotypes that occur following Ag exposure in vivo and that are also invariably accompanied by changes in the magnitude of the T cell response. Nevertheless, it would remain of interest in future studies to attempt to assess whether the so-called "quality" of such CD4$^+$ T cell responses affected efficacy in this blood-stage malaria model.

The AdHu5-MVA *P. chabaudi chabaudi* strain AS AMA1 immunization regimen described in this article was able to afford a level of protective efficacy against a *P. chabaudi chabaudi* strain AS blood-stage challenge that was only slightly less than that observed following immunization with recombinant AMA1 protein formulated in less clinically relevant adjuvants, such as Freund's or Montanide ISA720 (40, 43). This efficacy was measured as a significant reduction in peak parasitemia between the AMA1-vaccinated and control groups, but a similar rate of clearance occurred thereafter. In the literature, the early reduction in peak parasitemia in immunocompetent mice has been attributed to conformation-dependent anti-AMA1 Ab responses (31, 43), as well as CD4$^+$ T cell responses acting independently of Abs (31). The evidence in this study that vaccine-induced AMA1-specific CD4$^+$ T cells are capable of contributing to efficacy comes from
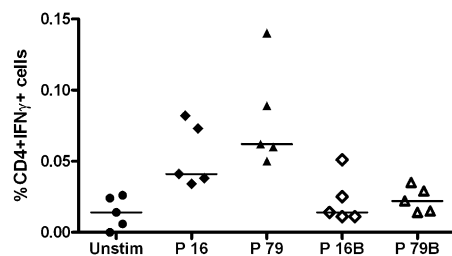
the significant loss of this antiparasitic effect in immunized mice following the depletion of CD4$^+$ T cells prior to *P. chabaudi chabaudi* strain AS pRBC challenge, whereas anti-AMA1–specific Ab titers remained unchanged postchallenge. These data concur with the observations of Xu et al. (31) but contrast with our previous studies in the *P. yoelii* MSP1$_{42}$ model, in which CD4$^+$ T cells were shown to provide essential help for priming B cells at the time of vaccination (7), but depletion of CD4$^+$ T cells prior to pRBC challenge failed to alter vaccine efficacy (9). The depletion experiments also suggested that *P. chabaudi chabaudi* strain AS AMA1-specific Abs, as well as those targeting other parasite Ags, are capable of contributing to parasite clearance. Despite similar levels of anti-parasite Abs, immunized and CD4$^+$ T cell-depleted mice were able to clear parasites faster than were their naive depleted counterparts. This enhanced rate of clearance was associated with higher levels of *P. chabaudi chabaudi* strain AS AMA1-specific Abs (induced by prior vaccination). However, in apparent contradiction of this, both the vaccinated and the naive nondepleted mice cleared their parasites at the same time, even though the naive mice possessed significantly lower levels of *P. chabaudi chabaudi* strain AS AMA1-specific Abs. These data suggest that both *P. chabaudi chabaudi* strain AS AMA1-specific Abs and Abs to other parasite Ags can contribute to parasite clearance, and they agree with other studies suggesting that the rate of infection resolution correlates with the level of malaria-specific Abs and the speed of their production (30). The data in this study suggest that the vaccine-induced anti-*P. chabaudi chabaudi* strain AS AMA1 Abs are capable of contributing to this critical threshold of total Ab that is necessary for parasite clearance but that Abs of other Ag specificities are just as effective.

The fact that *P. chabaudi chabaudi* strain AS AMA1-specific Abs were not detected in the naive CD4$^+$ T cell-depleted mice also suggests that CD4$^+$ T cell help is essential for production of *P. chabaudi chabaudi* strain AS AMA1-specific Abs. CD4$^+$ T cell help is also required for the production of Abs to other parasite Ags, because both the vaccinated and naive CD4$^+$ T cell-depleted mice showed significantly lower Abs postchallenge to the whole-parasite lysate in comparison with nondepleted mice. Previous data showing that CD4$^+$ T cells for a cryptic epitope in *P. chabaudi chabaudi* strain AS AMA1 (32), as well as an epitope in *P. chabaudi chabaudi* strain AS MSP1$_{33}$ (33), can prime anamnestic Ab responses to their respective Ags following challenge support this important role for CD4$^+$ T cell help for B cells.

Although transfer of immune sera alone into immunocompromised hosts is reported to be insufficient to control initial parasite densities (46), the studies that we performed showed that both vaccine-induced CD4$^+$ T cells and Abs can be adoptively transferred into naive immunocompetent mice, leading to significant

FIGURE 9. T cell response to heterologous AMA1 peptide sequences from other *P. chaubaudi* strains. BALB/c mice ($n = 5$) were primed with 1×10^{10} vp AdHu5-*P. chabaudi chabaudi* strain AS AMA1 and boosted 8 wk later with 1×10^7 PFU MVA-*P. chabaudi chabaudi* strain AS AMA1. Two weeks postboost (day 70), splenocytes were isolated and restimulated with peptides P16 and P79 (as described previously), with peptides P16B and P79B (heterologous peptides to P16 and P79, respectively), or no peptide (Unstim). Cells were surface stained for CD4, intracellularly stained for IFN-γ, and assessed by flow cytometry to determine the percentage of responding cells/total CD4$^+$ T cell subset. The figure shows the individual and median CD4$^+$ IFN-γ$^+$ responses.

control of initial peak parasitemia upon pRBC challenge. These data emphasize the fact that both arms of the immune system can play an important contributory role when functioning within an intact immune system. Although control sera failed to show this effect, there was an apparent intermediate (but not statistically significant) effect following transfer of CD4⁺ T cells from vector control-immunized mice. However, these data are in agreement with other studies showing that transfer of naive CD4⁺ T cells into immunodeficient mice can have a protective effect and that this is both cell number dependent (46) and, in some cases, less effective than transfer of parasite-specific CD4⁺ T cells (33). The ability of transferred cells to prolong and enhance the survival of nude mice again supports the importance of CD4⁺ T cells in mediating early control of parasite density in this model. Reduced potency in nude versus normal mice most likely reflects the overall lower absolute numbers of CD4⁺ T cells in the reconstituted nude mice. These experiments also did not dissect the contribution of naive versus *P. chabaudi chabaudi* strain AS AMA1-specific CD4⁺ T cells in the immunocompromised hosts, although it was shown that prior activation of such transferred T cell subsets (e.g., by vaccination with Ag following cell transfer but preceding pRBC challenge) may be necessary to tease apart these differences in protective capacity between naive and Ag-specific T cells (33).

A key rationale for developing such viral-vectored vaccines was the possibility of inducing T cell responses to conserved epitopes, which could aid in better induction of cross-strain immunity by AMA1 subunit vaccines (in contrast to the well-documented strain specificity of anti-AMA1 Ab responses) (12, 40, 47). When mice are immunized with recombinant *P. chabaudi chabaudi* DS AMA1 protein, it was shown that there is no heterologous protection against *P. chabaudi adami* 556KA (possessing an AMA1 sequence that differs by 36 aa) (40). Unfortunately, of the two CD4⁺ T cell epitopes identified in this model, both were polymorphic with respect to other strains of *P. chabaudi*. The failure to detect any T cell responses to the heterologous peptides (P16B and P17B) in *P. chabaudi chabaudi* strain AS AMA1-immunized mice or protection against challenge with heterologous parasite strains (Supplemental Fig. 3B) confirms that even a slight variation (2 aa) in the epitope sequence has a serious consequence with regard to immune recognition. The challenge data with *P. chabaudi adami* DK (in which only the P16 epitope is conserved) indicate that responses against the P79 epitope alone or combined with those against P16 are important for mediating efficacy (possibly in conjunction with strain-specific Abs). It is worth noting that, following immunization, responses were slightly stronger against P79, and it may be that responses against P16 alone were too weak to confer efficacy against the heterologous parasite. Nevertheless, this work was recently extended and similar viral-vectored vaccines were developed that target *P. falciparum* AMA1 and encode two alleles of AMA1 from the 3D7 and FVO strains. Importantly, following immunization of mice (12), rhesus macaques (9), and humans (14), T cell responses were measured against peptides that were conserved between the two alleles. Thus, if cell-mediated immunity contributes to parasite control in *P. falciparum* malaria in a similar fashion to that observed for *P. chabaudi*, then the induction of such responses may benefit the induction of better cross-strain immunity by such subunit vaccination strategies.

The data presented in this article were generated with a vaccine platform that is highly suited for human use, particularly with the substitution of a simian adenovirus for the human adenoviral vector (13, 14). They have important implications for the future development of subunit blood-stage malaria vaccines. If the protective immune mechanisms observed in the *P. chabaudi* model are also reflected in human immunity to blood-stage malaria, then the development of viral-vectored vaccines targeting Ags, such as *P. falciparum* AMA1, which induce strong cellular immune responses in conjunction with Abs, may stand a greater chance of success in protecting humans against blood-stage parasites in comparison with vaccination strategies aiming to induce Abs alone.

Disclosures

S.J.D., E.K.F., S.C.G., and A.V.S.H. are named inventors on patent applications covering malaria-vectored vaccines and immunization regimens. The other authors have no financial conflicts of interest.

References

1. Hill, A. V. 2011. Vaccines against malaria. *Philos. Trans. R. Soc. Lond. B Biol. Sci.* 366: 2806–2814.
2. Goodman, A. L., and S. J. Draper. 2010. Blood-stage malaria vaccines - recent progress and future challenges. *Ann. Trop. Med. Parasitol.* 104: 189–211.
3. Remarque, E. J., B. W. Faber, C. H. Kocken, and A. W. Thomas. 2008. Apical membrane antigen 1: a malaria vaccine candidate in review. *Trends Parasitol.* 24: 74–84.
4. Hirunpetcharat, C., J. H. Tian, D. C. Kaslow, N. van Rooijen, S. Kumar, J. A. Berzofsky, L. H. Miller, and M. F. Good. 1997. Complete protective immunity induced in mice by immunization with the 19-kilodalton carboxyl-terminal fragment of the merozoite surface protein-1 (MSP1[19]) of *Plasmodium yoelii* expressed in *Saccharomyces cerevisiae*: correlation of protection with antigen-specific antibody titer, but not with effector CD4+ T cells. *J. Immunol.* 159: 3400–3411.
5. Draper, S. J., and J. L. Heeney. 2010. Viruses as vaccine vectors for infectious diseases and cancer. *Nat. Rev. Microbiol.* 8: 62–73.
6. Hill, A. V., A. Reyes-Sandoval, G. O'Hara, K. Ewer, A. Lawrie, A. Goodman, A. Nicosia, A. Folgori, S. Colloca, R. Cortese, et al. 2010. Prime-boost vectored malaria vaccines: progress and prospects. *Hum. Vaccin.* 6: 78–83.
7. Draper, S. J., A. L. Goodman, S. Biswas, E. K. Forbes, A. C. Moore, S. C. Gilbert, and A. V. Hill. 2009. Recombinant viral vaccines expressing merozoite surface protein-1 induce antibody- and T cell-mediated multistage protection against malaria. *Cell Host Microbe* 5: 95–105.
8. Draper, S. J., S. Biswas, A. J. Spencer, E. J. Remarque, S. Capone, M. Naddeo, M. D. J. Dicks, B. W. Faber, S. C. de Cassan, A. Folgori, et al. 2010. Enhancing blood-stage malaria subunit vaccine immunogenicity in rhesus macaques by combining adenovirus, poxvirus, and protein-in-adjuvant vaccines. *J. Immunol.* 185: 7583–7595.
9. Draper, S. J., A. C. Moore, A. L. Goodman, C. A. Long, A. A. Holder, S. C. Gilbert, F. Hill, and A. V. Hill. 2008. Effective induction of high-titer antibodies by viral vector vaccines. *Nat. Med.* 14: 819–821.
10. Douglas, A. D., S. C. de Cassan, M. D. Dicks, S. C. Gilbert, A. V. Hill, and S. J. Draper. 2010. Tailoring subunit vaccine immunogenicity: maximizing antibody and T cell responses by using combinations of adenovirus, poxvirus and protein-adjuvant vaccines against *Plasmodium falciparum* MSP1. *Vaccine* 28: 7167–7178.
11. Goodman, A. L., C. Epp, D. Moss, A. A. Holder, J. M. Wilson, G. P. Gao, C. A. Long, E. J. Remarque, A. W. Thomas, V. Ammendola, et al. 2010. New candidate vaccines against blood-stage *Plasmodium falciparum* malaria: prime-boost immunization regimens incorporating human and simian adenoviral vectors and poxviral vectors expressing an optimized antigen based on merozoite surface protein 1. *Infect. Immun.* 78: 4601–4612.
12. Biswas, S., M. D. Dicks, C. A. Long, E. J. Remarque, L. Siani, S. Colloca, M. G. Cottingham, A. A. Holder, S. C. Gilbert, A. V. Hill, and S. J. Draper. 2011. Transgene optimization, immunogenicity and in vitro efficacy of viral vectored vaccines expressing two alleles of *Plasmodium falciparum* AMA1. *PLoS ONE* 6: e20977.
13. Sheehy, S. H., C. J. Duncan, S. C. Elias, K. A. Collins, K. J. Ewer, A. J. Spencer, A. R. Williams, F. D. Halstead, S. E. Moretz, K. Miura, et al. 2011. Phase Ia clinical evaluation of the *Plasmodium falciparum* blood-stage antigen MSP1 in ChAd63 and MVA vaccine vectors. *Mol. Ther.* 19: 2269–2276.
14. Sheehy, S. H., C. J. A. Duncan, S. C. Elias, S. Biswas, K. A. Collins, G. A. O'Hara, F. D. Halstead, K. J. Ewer, T. Mahungu, A. J. Spencer, et al. 2012. Phase Ia Clinical Evaluation of the Safety and Immunogenicity of the *Plasmodium falciparum* Blood-Stage Antigen AMA1 in ChAd63 and MVA Vaccine Vectors. *PLoS ONE* 7: e31208.

15. Reyes-Sandoval, A., T. Berthoud, N. Alder, L. Siani, S. C. Gilbert, A. Nicosia, S. Colloca, R. Cortese, and A. V. Hill. 2010. Prime-boost immunization with adenoviral and modified vaccinia virus Ankara vectors enhances the durability and polyfunctionality of protective malaria CD8+ T-cell responses. *Infect. Immun.* 78: 145–153.

16. Reyes-Sandoval, A., S. Sridhar, T. Berthoud, A. C. Moore, J. T. Harty, S. C. Gilbert, G. Gao, H. C. Ertl, J. C. Wilson, and A. V. Hill. 2008. Single-dose immunogenicity and protective efficacy of simian adenoviral vectors against *Plasmodium berghei*. *Eur. J. Immunol.* 38: 732–741.

17. Goodman, A. L., A. M. Blagborough, S. Biswas, Y. Wu, A. V. Hill, R. E. Sinden, and S. J. Draper. 2011. A viral vectored prime-boost immunization regime targeting the malaria Pfs25 antigen induces transmission-blocking activity. *PLoS ONE* 6: e29428.

18. Good, M. F., and C. Engwerda. 2011. Defying malaria: Arming T cells to halt malaria. *Nat. Med.* 17: 49–51.

19. Pombo, D. J., G. Lawrence, C. Hirunpetcharat, C. Rzepczyk, M. Bryden, N. Cloonan, K. Anderson, Y. Mahakunkijcharoen, L. B. Martin, D. Wilson, et al. 2002. Immunity to malaria after administration of ultra-low doses of red cells infected with *Plasmodium falciparum*. *Lancet* 360: 610–617.

20. Roestenberg, M., M. McCall, J. Hopman, J. Wiersma, A. J. Luty, G. J. van Gemert, M. van de Vegte-Bolmer, B. van Schaijk, K. Teelen, T. Arens, et al. 2009. Protection against a malaria challenge by sporozoite inoculation. *N. Engl. J. Med.* 361: 468–477.

21. Kawabata, Y., H. Udono, K. Honma, M. Ueda, H. Mukae, J. Kadota, S. Kohno, and K. Yui. 2002. Merozoite surface protein 1-specific immune response is protective against exoerythrocytic forms of *Plasmodium yoelii*. *Infect. Immun.* 70: 6075–6082.

22. Belnoue, E., T. Voza, F. T. Costa, A. C. Grüner, M. Mauduit, D. S. Rosa, N. Depinay, M. Kayibanda, A. M. Vigário, D. Mazier, et al. 2008. Vaccination with live *Plasmodium yoelii* blood stage parasites under chloroquine cover induces cross-stage immunity against malaria liver stage. *J. Immunol.* 181: 8552–8558.

23. Imai, T., J. Shen, B. Chou, X. Duan, L. Tu, K. Tetsutani, C. Moriya, H. Ishida, S. Hamano, C. Shimokawa, et al. 2010. Involvement of CD8+ T cells in protective immunity against murine blood-stage infection with *Plasmodium yoelii* 17XL strain. *Eur. J. Immunol.* 40: 1053–1061.

24. Wipasa, J., C. Hirunpetcharat, Y. Mahakunkijcharoen, H. Xu, S. Elliott, and M. F. Good. 2002. Identification of T cell epitopes on the 33-kDa fragment of *Plasmodium yoelii* merozoite surface protein 1 and their antibody-independent protective role in immunity to blood stage malaria. *J. Immunol.* 169: 944–951.

25. Stevenson, M. M., and E. M. Riley. 2004. Innate immunity to malaria. *Nat. Rev. Immunol.* 4: 169–180.

26. Langhorne, J. 1989. The role of CD4+ T-cells in the immune response to *Plasmodium chabaudi*. *Parasitol. Today (Regul. Ed.)* 5: 362–364.

27. Taylor-Robinson, A. W. 2010. Regulation of immunity to *Plasmodium*: implications from mouse models for blood stage malaria vaccine design. *Exp. Parasitol.* 126: 406–414.

28. Mosmann, T. R., H. Cherwinski, M. W. Bond, M. A. Giedlin, and R. L. Coffman. 2005. Two types of murine helper T cell clone. I. Definition according to profiles of lymphokine activities and secreted proteins. 1986. *J. Immunol.* 175: 5–14.

29. Mosmann, T. R., and R. L. Coffman. 1989. TH1 and TH2 cells: different patterns of lymphokine secretion lead to different functional properties. *Annu. Rev. Immunol.* 7: 145–173.

30. von der Weid, T., D. Kitamura, K. Rajewsky, and J. Langhorne. 1994. A dual role for B cells in *Plasmodium chabaudi chabaudi* (AS) infection? *Res. Immunol.* 145: 412–419.

31. Xu, H., A. N. Hodder, H. Yan, P. E. Crewther, R. F. Anders, and M. F. Good. 2000. CD4+ T cells acting independently of antibody contribute to protective immunity to *Plasmodium chabaudi* infection after apical membrane antigen 1 immunization. *J. Immunol.* 165: 389–396.

32. Amante, F. H., P. E. Crewther, R. F. Anders, and M. F. Good. 1997. A cryptic T cell epitope on the apical membrane antigen 1 of *Plasmodium chabaudi adami* can prime for an anamnestic antibody response: implications for malaria vaccine design. *J. Immunol.* 159: 5535–5544.

33. Stephens, R., F. R. Albano, S. Quin, B. J. Pascal, V. Harrison, B. Stockinger, D. Kioussis, H. U. Weltzien, and J. Langhorne. 2005. Malaria-specific transgenic CD4(+) T cells protect immunodeficient mice from lethal infection and dem-

34. Pinzon-Charry, A., V. McPhun, V. Kienzle, C. Hirunpetcharat, C. Engwerda, J. McCarthy, and M. F. Good. 2010. Low doses of killed parasite in CpG elicit vigorous CD4+ T cell responses against blood-stage malaria in mice. *J. Clin. Invest.* 120: 2967–2978.

35. McCarthy, J. S., and M. F. Good. 2010. Whole parasite blood stage malaria vaccines: a convergence of evidence. *Hum. Vaccin.* 6: 114–123.

36. Roestenberg, M., E. Remarque, E. de Jonge, R. Hermsen, H. Blythman, O. Leroy, E. Imoukhuede, S. Jepsen, O. Ofori-Anyinam, B. Faber, et al. 2008. Safety and immunogenicity of a recombinant *Plasmodium falciparum* AMA1 malaria vaccine adjuvanted with Alhydrogel, Montanide ISA 720 or AS02. *PLoS ONE* 3: e3960.

37. Forbes, E. K., S. Biswas, K. A. Collins, S. C. Gilbert, A. V. Hill, and S. J. Draper. 2011. Combining liver- and blood-stage malaria viral-vectored vaccines: investigating mechanisms of CD8+ T cell interference. *J. Immunol.* 187: 3738–3750.

38. Roederer, M., J. L. Nozzi, and M. C. Nason. 2011. SPICE: exploration and analysis of post-cytometric complex multivariate datasets. *Cytometry A* 79: 167–174.

39. Sinden, R. E., G. A. Butcher, and A. L. Beetsma. 2002. Maintenance of the *Plasmodium berghei* life cycle. *Methods Mol. Med.* 72: 25–40.

40. Crewther, P. E., M. L. Matthew, R. H. Flegg, and R. F. Anders. 1996. Protective immune responses to apical membrane antigen 1 of *Plasmodium chabaudi* involve recognition of strain-specific epitopes. *Infect. Immun.* 64: 3310–3317.

41. Bruña-Romero, O., G. González-Aseguinolaza, J. C. Hafalla, M. Tsuji, and R. S. Nussenzweig. 2001. Complete, long-lasting protection against malaria of mice primed and boosted with two distinct viral vectors expressing the same plasmodial antigen. *Proc. Natl. Acad. Sci. USA* 98: 11491–11496.

42. Darrah, P. A., D. T. Patel, P. M. De Luca, R. W. Lindsay, D. F. Davey, B. J. Flynn, S. T. Hoff, P. Andersen, S. G. Reed, S. L. Morris, et al. 2007. Multifunctional TH1 cells define a correlate of vaccine-mediated protection against *Leishmania major*. *Nat. Med.* 13: 843–850.

43. Anders, R. F., P. E. Crewther, S. Edwards, M. Margetts, M. L. Matthew, B. Pollock, and D. Pye. 1998. Immunisation with recombinant AMA-1 protects mice against infection with *Plasmodium chabaudi*. *Vaccine* 16: 240–247.

44. Qin, S., S. Cobbold, H. Tighe, R. Benjamin, and H. Waldmann. 1987. CD4 monoclonal antibody pairs for immunosuppression and tolerance induction. *Eur. J. Immunol.* 17: 1159–1165.

45. Taylor-Robinson, A. W., and R. S. Phillips. 1994. B cells are required for the switch from Th1- to Th2-regulated immune responses to *Plasmodium chabaudi chabaudi* infection. *Infect. Immun.* 62: 2490–2498.

46. Cavacini, L. A., C. A. Long, and W. P. Weidanz. 1986. T-cell immunity in murine malaria: adoptive transfer of resistance to *Plasmodium chabaudi adami* in nude mice with splenic T cells. *Infect. Immun.* 52: 637–643.

47. Thera, M. A., O. K. Doumbo, D. Coulibaly, M. B. Laurens, A. Ouattara, A. K. Kone, A. B. Guindo, K. Traore, I. Traore, B. Kouriba, et al. 2011. A field trial to assess a blood-stage malaria vaccine. *N. Engl. J. Med.* 365: 1004–1013.

48. Hodder, A. N., P. E. Crewther, and R. F. Anders. 2001. Specificity of the protective antibody response to apical membrane antigen 1. *Infect. Immun.* 69: 3286–3294.

49. Ouattara, A., J. Mu, S. Takala-Harrison, R. Saye, I. Sagara, A. Dicko, A. Niangaly, J. Duan, R. D. Ellis, L. H. Miller, et al. 2010. Lack of allele-specific efficacy of a bivalent AMA1 malaria vaccine. *Malar. J.* 9: 175.

50. Sullivan, N. J., T. W. Geisbert, J. B. Geisbert, L. Xu, Z. Y. Yang, M. Roederer, R. A. Koup, P. B. Jahrling, and G. J. Nabel. 2003. Accelerated vaccination for Ebola virus haemorrhagic fever in non-human primates. *Nature* 424: 681–684.

51. de Cassan, S. C., E. K. Forbes, A. D. Douglas, A. Milicic, B. Singh, P. Gupta, V. S. Chauhan, C. E. Chitnis, S. C. Gilbert, A. V. Hill, and S. J. Draper. 2011. The requirement for potent adjuvants to enhance the immunogenicity and protective efficacy of protein vaccines can be overcome by prior immunization with a recombinant adenovirus. *J. Immunol.* 187: 2602–2616.

52. Sridhar, S., A. Reyes-Sandoval, S. J. Draper, A. C. Moore, S. C. Gilbert, G. P. Gao, J. M. Wilson, and A. V. Hill. 2008. Single-dose protection against *Plasmodium berghei* by a simian adenovirus vector using a human cytomegalovirus promoter containing intron A. *J. Virol.* 82: 3822–3833.

onstrate requirement for a protective threshold of antibody production for parasite clearance. *Blood* 106: 1676–1684.